Orbit Stability and Feedback Control in Synchrotron Radiation Rings *

L. H. Yu
National Synchrotron Light Source,
Brookhaven National Laboratory, Upton NY11973

Abstract

Stability of the electron orbit is essential for the utilization of a low emittance storage ring as a high brightness radiation source. We discuss the development of the measurement and feedback control of the closed orbit, with emphasis on the activities at the National Synchrotron Light Source of BNL. We discuss the performance of the beam position detectors in use and under development: the PUE RF detector, split ion chamber detector, photo-emission detector, solid state detector, and the graphite detector. Depending on the specific experiments, different beamlines require different tolerances on the orbit motion. Corresponding to these different requirements, we discuss two approaches to closed orbit feedback: the global and local feedback systems. Then we describe a new scheme for the real time global feedback by implementing a feedback system based upon a harmonic analysis of both the orbit movements and the correction magnetic fields.

1. Introduction

Orbit stability is critical for high brightness synchrotron facilities. In recent years more and more synchrotron radiation sources are being developed through out the world. The trend of development is toward smaller emittance, hence smaller electron beam size and higher brightness. Orbit stability must also be improved correspondingly to take full advantage of low emittance and smaller beam size. As summarized from a user survey, a rule of thumb is that if the rms beam movement is less than 10 - 20 % of the rms beam size σ_z, it would be satisfactory for most experimental beamlines.

However, without closed orbit feedback, this requirement can not be achieved, because beam motion due to all sorts of noise sources is comparable to the beam size. Therefore, the development of feedback systems is very important for optimizing the performance of synchrotron radiation sources. As an example, we consider a beamline with imaging optics, where the image of the electron beam is projected onto an entrance slit. This type of system, such as the spherical grating monochromator on beamline U4 at NSLS, is very sensitive to beam motion. If the slit initially is aligned on the peak of the beam profile, its intensity fluctuation ΔI due to a beam movement of Δz, is given by $\frac{\Delta I}{I} = 1 - \exp^{\frac{\Delta z^2}{2\sigma_z^2}}$. In Table 1, we list this dependence as a reference, with $\sigma_z \approx 100\mu m$.

Table 1

Δz	$\frac{\Delta I}{I}$
$\pm 10\mu$	0.5%
$\pm 20\mu$	2%
$\pm 50\mu$	12%
$\pm 100\mu$	40%

This table shows that even a moderate improvement of the orbit stability from $\pm 50\mu m$ to $\pm 20\mu m$, will reduce the intensity fluctuation from 12% down to 2%, a significant improvement.

To solve the orbit stability problem, the first requirement is to be able to measure orbit position reliably to high precision. A beam position can be judged by the following properties:

(1). The beam position signal should be independent of the current in the storage ring, otherwise the current change could be mistaken as a beam movement. Our detailed analysis of a split ion chamber[1] shows that to eliminate the apparent beam motion due to beam current changes, the leakage current, matching of the gains of amplifiers, the zero points of the amplifiers and dividers, etc., all need delicate adjustment. And the nonlinearity of the relationship between the beam current and detector signal introduces an apparent beam motion, this apparent motion becomes null only when the beam is located at the electrical center of the detector. This is not unique to the split ion chamber, but is common to many other types of detectors

(2). The long term drift of the beam position zero point offset should be small, because this can be confused as a fictitious beam motion.

(3). The bandwidth of the detector should be larger than the bandwidth of the steering magnet power drive to be used for feedback. The later is usually limited by the eddy current of the vacuum chamber to a few hundred Hz. Otherwise when the detector is used in an orbit feedback system the speed of the feedback system will be limited by the detector.

(4). High position resolution, which is determined by the detector noise within the feedback system bandwidth. The detector noise can be characterized by the noise per square root of bandwidth. This, combined with the bandwidth of the feedback system, determines the noise contributed by the detector to the system. Clearly the noise within the system bandwidth will limit the ultimate orbit stability a feedback system can provide.

(5). Wide dynamical range in beam position. If the beam moves out of the dynamic range of a detector, which is a part of an orbit feedback system, the system will fail. We prefer this dynamic range to be larger than the maximum beam movement range. This condition can be met by electron beam position monitors, but is unlikely to be satisfied by photon beam monitors.

(6). Large dynamical range in beam current. The detector should be able to stand the highest beam current, while maintaining low noise level in the low current limit.

(7). Low cost. Especially when the detector is to be mass produced.

In this paper we will discuss several types of beam position monitors that are being developed at the NSLS. For the electron beam position monitor, we will discuss a PUE RF receiver, which is designed to improve resolution and lower cost. This detector has recently been used in our harmonic

*This work has been performed under the auspices of the U.S. Department of Energy.

CH2669-0/89/0000-0054$01.00©1989 IEEE

global closed orbit feedback system, and will be used for fast orbit display. As examples of monitors observing the photon beam we discuss: split ion chamber, photo-emission detector, solid state detector, graphite detector.

To solve the orbit stability problem, the next requirement is the development of feedback systems. These include the local bump systems and the global feedback system, and the proper combination of them.

The local bump feedback system has been developed by R. Hettel at SRRL[2]. It is a well established technique, and can reduce the beam movement by a factor of 10 - 100 at one beam line. For certain beamlines it is a necessary tool. It has been a general practice to install local bump feedback systems for the beamlines with the tightest beam movement tolerances, and still more local bump feedback systems are being developed at NSLS. We will describe the basic configurations of these systems.

However, to install local bump feedback systems for every beamline at NSLS is both costly and impractical. There are nearly 100 beamlines crowded around the X-raing and UV ring. Every local bump feedback system needs 3 - 4 steering magnets and 1 - 2 detectors, it is clear that for such a crowded arrangement of beamlines, it will need a large number of detectors and trim magnets to install local bumps for every beamline. Aside from the cost of installation and maintenance, there is not enough space in the ring for more steering magnets. The condition for the locality is very critical, it requires accurate ratios between the strengths of the steering magnets. The tiny residual of non-locality may cause couplings between different local bump feedback loops, and may introduce oscillation. The steering magnets in a local bump have opposite signs to keep the steering local, so the magnets are actually fighting each other, thus requiring large magnet strength to correct large beam motion. Sometimes large beam motion can cause the steering magnets to go out of range. Global orbit correction is a very effective method to overcome these limitations.

Digital global orbit correction control programs are used in almost every accelerator. For example, KEK has installed a digital global orbit control system to correct orbit motion every few minutes. This is a slow process, the beam motion between two corrections can not be stabilized, and can greatly reduce the precision of the correction because the measurement can not be more precise than the beam movement during the measurements. To improve this, we are developing a real time harmonic global feedback system at the NSLS. This system corrects the Fourier components of the orbit nearest to the betatron tune. As compared to the stability improvement of a factor of 10 to 100 at one beamline by a local bump feedback system, the present harmonic feedback system improves the orbit stability by a factor of 3 to 4 everywhere around the storage ring, thus providing the required beam stability for most beamlines. The effort required is about the same as for one local bump feedback system. For the beamlines with the tightest beam stability requirement, local bump feedback can still be added, with much reduced steering magnet strengths. The harmonic feedback system fully uses the fact that the orbit distortion is dominated by its harmonic components nearest to the tune, so the position signals from different detectors are correlated, hence the harmonic feedback system also improves the signal to noise ratio.

In the following we will discuss the activities on the orbit stability problem in NSLS. First, in section 2, we will describe the beam motion observed at NSLS, taking the UV ring as an example. In section 3 we will discuss the development of position monitors.

In section 4 we will discuss the feedback systems. First we discuss the basic configurations of the local bump system, and some experiences gained during their development at NSLS. Then we describe the basic principles of the real time harmonic feedback system, and some recent experimental results.

2. Orbit Movement

Observations of orbit variation that exceed desirable tolerances, sometimes to an intolerable degree in the vertical plane (where the beam misses the experiment altogether), have been reported at many SR laboratories[2]. We consider the UV ring of NSLS as an example. The vertical beam size $\sigma \approx 200\mu$. The beam motion is quite complicated, consisting of many different frequencies, and the behavior changes from time to time. Sometimes it is very quiet, sometimes it can reach a level even larger than the beam size. Some of the noise sources have been located, others are still unknown. Table 2 gives a rough idea of how large the beam motion can be. The most detrimental beam movement has a characteristic time scale of minutes, sometimes the beam is very quiet, sometimes there is a very irregular movement as large as $\pm 50\mu m$ to $\pm 70\mu m$. The beam position occasionally also experiences a sudden shift of about $100\mu m$. A beam motion with a period of about 10 minutes and an amplitude of about $\pm 30\mu m$ is identified as due to the temperature fluctuation of the cooling water.

Table 2

fill to fill (range)	drift within fill (range)	1 min (range)	$\frac{1}{f}$ noise (< 10Hz) (rms)	Booster noise (0.6Hz) (rms)	AC 60,.., 360 Hz (rms)
400μ	200μ	100μ	±10μ	±10μ	±12μ

These data indicate the importance of the orbit stability problem. Obviously, it would be the best if one could locate the noise sources and eliminate them. However, this is very difficult, hence the development of feedback systems becomes necessary.

3. Beam Position Monitors

M. Billing has given a comprehensive review on the beam position monitors [3]. Here we will limit our discussion to beam position monitors under development at the NSLS. For the electron BPM, we briefly discuss the PUE RF receiver. This has been widely used in accelerators. The development at the NSLS is aimed at increasing the speed, improving the resolution, and lowering the cost, so it can be mass produced to be used in global feedback systems, the fast display of the orbit and interlock systems, etc. For the photon BPM, we first discuss the split ion chamber, which has been used at NSLS to study the apparent beam motion due to the beam current changes. Then we discuss the photo-emission detector, which is used for local feedback on the soft X-ray beamlines. We will briefly describe one of its new versions with very low noise developed at NSLS. Finally, we discuss some efforts at NSLS for new types of detectors such as a solid state detector and a graphite detector which are aimed at low cost, simplicity and wide dynamic range.

3.1 PUE RF Receiver

The PUE detector utilizes the image charge induced by the electron bunches. The signal from the electrode consists of the harmonics of the revolution frequency of the electron bunch. The signal strengths (A,B,C,D) from the electrodes depend on their distances from the electron beam, thus determining the beam position. The vertical beam position relative to the geometrical center of the 4 electrodes of one PUE station is given by:

$$z = K \quad \frac{(A+B) - (C+D)}{A+B+C+D}$$

The PUE monitor is widely used in accelerators to monitor the global orbit. At NSLS one RF receiver is used to monitor all the PUE stations by scanning though a tree of switches, and is very slow. A new RF receiver is being developed to replace this tree system so that every PUE station has its own dedicated RF receiver, thus providing fast orbit display.

The PUE RF receiver developed at NSLS is described in a separate paper by J. Bittner and R. Biscardi in this conference [4]. So we will only give a brief description here (see fig.1). The signals from the 4 electrodes usually require four amplifiers and detectors with gains matched very closely over a very wide dynamic range. This requires very careful calibration of components and is difficult to achieve and maintain. The problem is solved by measuring only one Fourier component of the signal and by "time sharing" a single amplifier and detector among the 4 button electrodes. The "time sharing" is achieved by using two sets of synchronized fast switches before and after the RF amplifier and detector. All four buttons are sampled at a 40kHz repetition frequency. The output bandwidth is limited to 300 Hz. The sum signal is used for a slow automatic control of the amplifier gain such that the sum signal remains constant. This servo control keeps the amplifier and detector in a very limited and linear part of its dynamic range. As a result, the dynamic range in current is about 30dB. Within this range the noise level is kept at 40 $\mu V/\sqrt{Hz}$, and the noise within the 300Hz bandwidth is $\pm 3\mu$. A commercially available TV detector is used. The constant sum signal makes an accurate divider unnecessary, because the denominator is a constant. The switch used is a GaAs switch, which is very fast (rise time in the order of ns), and needs very small driving current to control the switching, so the driving circuit is also simplified, and the radiation noise during switching is reduced.

Because of this detector's high speed, low noise, wide position dynamic range, wide current dynamic range, and its low cost, it is being mass produced at NSLS. It will be used in our global feedback system, fast orbit display, and interlock systems.

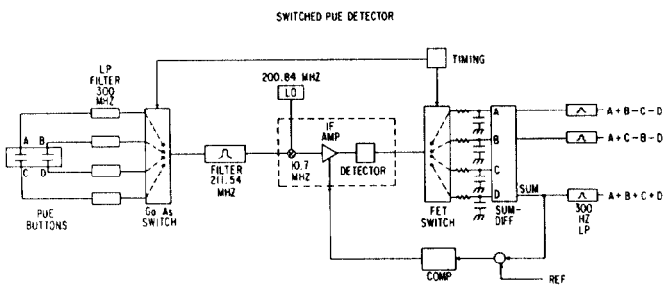

fig.1

3.2 Split Ion Chamber

In an ion chamber[5], the synchrotron light passes between vertically mounted anode and cathode plates. The ion chamber is filled with flowing gas (we used both helium and nitrogen gas). The anode is split diagonally into two triangular plates (see fig.2). The ionization current sensed by the upper and lower anode plates depends on the height of the synchrotron light beam. The difference divided by the sum of these two current signals is proportional to the deviation of the beam from the center.

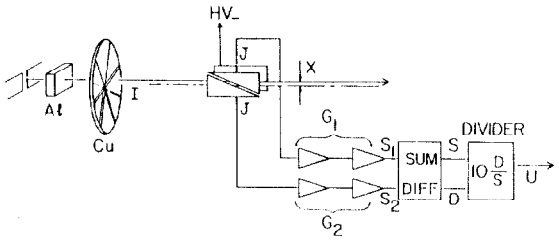

fig.2

Ion chambers are widely used in local bump feedback systems. For hard X-ray beamlines, it is non-destructive, and can be used in line with the experimental station.

Our ion chamber, serving as a beam position monitor, indicated a relation between the beam position and the beam current. This current position dependence was also reported from other types of detectors, for example, solid state detectors. As a result it was generally believed that right after injection, when the current was high, the beam moved to one direction, and as the current decayed the beam gradually moved in the other direction. To verify this, we studied the intensity dependence of the ion chamber by setting up a rotating wheel with several partitions with different thickness of copper in front of the ion chamber to vary the attenuation of the radiation intensity[1]. Our study concluded that most of this apparent beam motion was due to the ion chamber itself. By carefully matching the gains of the two amplifiers, adjusting both the input and output offsets of the divider, compensating the very small leakage currents of the anodes plates, and properly selecting the attenuation to reduce the nonlinearity due to the recombination process of the ions and electrons, we reduced the current dependence to below 5μ within $\pm 500\mu$ dynamic range. With this intensity independent ion chamber monitor, we observed the long term beam motion, the result shows that most of the long term beam drift is independent of the beam current. As can be seen from fig.3 , there is clearly a position continuity before and after a fill, even though the current changed from the minimum to the maximum right after injection. Hence a suspicion that the long term beam movement is caused by the heating due to the synchrotron radiation at high current was cleared. Using this ion chamber as a tool to check other detectors, we found that the solid state detector's leakage current caused the apparent beam motion.

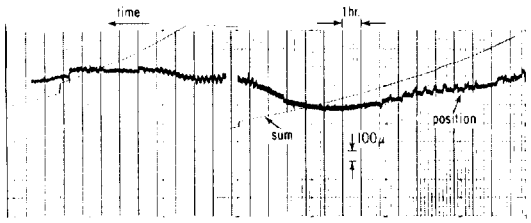

fig.3

3.3 Photo-emission Detector

In a photo-emission detector[6], the outer edge of the synchrotron light beam profile is intercepted by two pairs of tungsten blades (see fig.4) The environment is biased positively relative to the blades, so the photo-electrons from the blades are pulled away to reduce cross talk. The vertical beam position is calculated from the difference in photo-emission currents between the upper and lower blades. The center part of the radiation passes the detector uninterrupted, so this detector is widely used in line with the experimental station, providing feedback signals for local bump feedback systems. The blades are water cooled so the detector can stand high flux of synchrotron radiation.

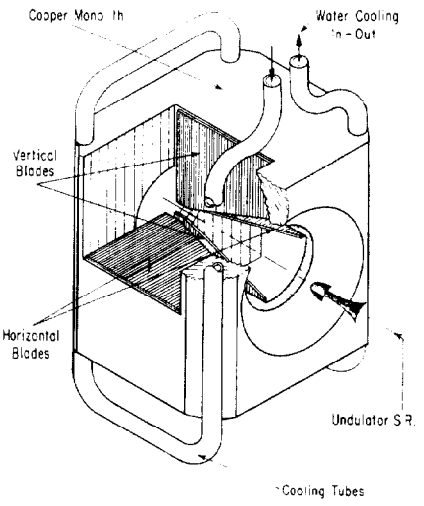

fig.4

However, the photo-emission detector operates in ultra high vacuum, the blades are very thin and very sensitive to alignment errors, making this device expensive and difficult to be assemble and align. The photo-yield is sensitive to surface composition and contamination which can be modified by exposure to radiation. This sometimes influences the reproducibility of the beam position measurement. Another disadvantage of this detector is its small position dynamic range. The upper and lower blades are separated by about 2σ of the vertical beam size at the monitor site, if the beam moves more than a few σ away from the center, the monitor may lose track of the beam position. So after injection, if the beam moves too far, the local bump feedback system loop can not be closed, and orbit correction is required before the loop can be closed.

The detector shown in fig.4 is a new version of photoemission detector, developed at NSLS[7]. In this detector, the horizontal and vertical blades are symmetrically mounted on a water cooled copper monolith. The blades are insulated from the monolith by beryllia shims, which is a good insulator electrically , and also a good heat conductor. This structure insured a efficient water cooling without introducing vibration from the cooling water. The monolith is biased to +300V with the signal blades near ground level. This provides excellent electrical shielding, and results in a very low noise level of about 0.1μ. The fact that there is no individual control of the four blades simplifies the assembly and alignment of this detector.

During the installation of a local bump feedback system on a soft X-ray undulator beamline with a photo-emission monitor, R. Nawrocky et el observed a 40% coupling between the vertical and horizontal motion. They found that this results from the interference of the nearby bending magnet radiation with the soft X-ray undulator radiation. The radiation from the bending magnet increases the photocurrent of the lower blade, hence even when the undulator radiation is centered, the position signal indicates the beam is low. When the undulator radiation beam moves horizontally away from the center of the detector, the relative weight of the dipole radiation over the undulator radiation increases, and the vertical position signal moves downward. This problem is due to the fact that the detector can not distinguish hard and soft X-rays. One idea is to use material for the blades selected to make it more sensitive to the soft X-rays than hard X-rays[8]. For example, the tungsten blades can be coated with graphite, which is more sensitive to the soft X-rays but is almost transparent to hard X-rays.

3.4 Solid State Detector and Graphite Detector

Motivated by the geometric configuration of the split ion chamber, P. Siddons and H. Kraner tested a solid state position detector[9]. A square PIN photodiodes active area is split diagonally to give two triangular elements. When the X-ray beam from a dipole source impinges on the diode at normal incidence, the trace of the beam is a horizontal line. The photocurrent generated in each diode is proportional to the illuminated area. Again the vertical beam position is determined by the difference of the two current signals divided by the sum. A 6 mm aluminum filter is used to reduce the power deposited in the diode. At a beam current of 10mA, the resolution, determined by the electronic noise, is 1 micron. To eliminate the apparent beam motion due to the current changes, the leakage current of the photodiodes should be carefully compensated by the offset of the amplifiers. However, after a few weeks exposure to the X-ray beam, the leakage current changes because of radiation damage. Consequently the leakage currents should be regularly monitored and compensated, if it is to be used as a reliable source of beam position information. A scheme to carry this out is under way.

To avoid the radiation damage problem, E. Johnson replaced the photodiodes in the above solid state detector by graphite plates, and tested it as a photo-emission detector. The noise is at submicron level, and the position dynamic range is as good as that of a split ion chamber detector. Because of the low Z of graphite, the detector is transparent to hard X-rays, so it can also be used in line with experimental beamlines, and for the same reason, the power deposition in the graphite is small, so there is no need for a cooling system. The device is very simple, and cost is low. This detec-

tor combines the advantages of several other detectors, and has a promising future. Further development is in progress.

4. Closed Orbit Feedback Systems

4.1 Local Bump Feedback System

R. Hettel has given a comprehensive review of local bump feedback systems[2]. Here we only briefly describe the basic configurations and some experience gained at the NSLS during the implementation of local bump feedback[10].

The basic buiding block of a local bump is based on utilizing three magnets. To insure the locality, the three steering magnet strengths must have a fixed ratio, so there is only one free parameter, i.e. the amplitude of the local bump. This parameter is determined by one detector on the beamline. The feedback system keeps the radiation beam centered at the detector. If the experimental station is very close to the detector, and far from the radiation source, then the beam position at the experimental station is also stabilized. In this system the beam position and angle cannot be independently controlled.

When both angle and position need to be controlled independently, we need a superposition of two sets of three trim local bumps. The two local bumps can share two trims, so the system uses 4 trim magnets. The amplitudes of the two local bumps are two independent parameters, so we need two detectors to control them. One should be close to the source point, for example, it can be a PUE RF detector, the other detector should be close to the experimental station, for example, it can be a photo-emission detector. When the feedback system loop is closed, the beam is fixed at the centers of both detectors, and both angle and position are stabilized. A four trim feedback system of this type has been operated successfully at U15 beamline of NSLS[11]. Several others are in progress.

One experience gained during the installation of local bumps at NSLS is that d[illegible]nt trims may have different frequency responses, thus when the trim strength ratio is adjusted to make the bump local at low frequency, at higher frequencies the ratio changes so the locality can be violated[10]. For example, the local bump feedback system developed for the X-1 beamline at NSLS has 4 trims, 2 of which are close to aluminum vacuum chamber, with the other two between aluminum and stainless vacuum chambers. As a result the first two trims have much lower bandwidth than the other two. This resulted in a very abnormal frequency response curve for the local bump, and for high frequency the bump is not local. By careful frequency compensation, the frequency response curves of the four trims are matched and the bump is localized.

4.2 Real Time Harmonic Feedback System

The harmonic global orbit correction uses the fact that the orbit distortion is dominated by its harmonic components nearest to the tune. To carry out a harmonic orbit correction, we first measure the orbit, then Fourier analyze its displacements. To implement real time harmonic feedback, the problem is how to use a limited number of detectors and trims to realize this process. We have developed a scheme to accomplish this task[12]. The experiment based on this scheme is given in a separate paper in this conference[13]. Here we give a brief description.

Even with a very limited number of detectors (e.g., 4 detectors in the UV ring), the Fourier analysis can be done by a simple linear analog network. The input voltages are proportional to the orbit displacements at the detectors, and in real time the output voltages are proportional to the desired Fourier harmonic coefficients. Another linear analog network can be built to generate desired orbit with required Fourier coefficients, even with a limited number of steering magnets (e.g. 4 trims in the UV ring). The input voltages are proportional to the desired Fourier coefficients, the output voltages are proportional to the required trim currents to generate the desired orbit distortion. When these two networks are connected by servo circuits, the Fourier components in the orbit distortion are forced to vanish.

To carry out the Fourier analysis, we use the least square method to fit the output of the detectors, assuming the approximation that the orbit can be represented by the sum of a few harmonics nearest to the tune.

For a single noise source at phase ϕ_0, the orbit distortion is

$$\eta = t\cos\nu(\pi - |\phi - \phi_0|) \quad . \tag{4.1}$$

Here η and ϕ are Courant-Snyder's scaled orbit displacement ($\eta = y/\sqrt{\beta}$), and betatron oscillation phase respectively[14]. ν is the tune, and t is scaled noise strength.

As an example, the NSLS UV ring has a vertical tune of 1.2, and the first harmonic component dominates,. We can approximately write:

$$\eta \approx a\ \cos\phi + b\ \sin\phi. \tag{4.2}$$

There are only two unknown Fourier coefficients a and b, and in principle only the displacements at two locations need to be determined to calculate a and b. When we have 4 detectors, we can use a least square method to calculate a and b. When there are only two detectors, they must be separated by nearly $\pi/2$ phase advance to maximize the determinant of the equations, so they cannot be distributed uniformly. When there are 4 detectors we can distribute them uniformly around the ring so the orbit improvement is more uniform around the ring. The redundancy of detectors also improves the accuracy, because the correlation between the signals from different detectors enhances the signal to noise ratio. The result is, in terms of matrix notation[12]:

$$\begin{bmatrix} a \\ b \end{bmatrix} = \mathbf{F} \begin{bmatrix} \eta_1 \\ \eta_2 \\ \eta_3 \\ \eta_4 \end{bmatrix} \tag{4.3}$$

Here η_i's are the displacements at the 4 detectors, F is a matrix which is completely determined by the phases of the detectors. It is noted that these phases are known quite accurately, particularly when the ring has a 4 -fold symmetry (4 superperiods), as is the case for the UV ring. If the 4 detectors are periodically distributed around the ring, the phase advance of two detectors next each other is exactly $\pi/2$. Clearly, the matrix operation (4.3) can be carried out by a simple linear analog circuit F.

In a similar way, the trim strengths required to generate an orbit with Fourier coefficients -a and -b can be calculated by a matrix multiplication:

$$\begin{bmatrix} t_1 \\ t_2 \\ t_3 \\ t_4 \end{bmatrix} = \mathbf{T} \begin{bmatrix} -a \\ -b \end{bmatrix} \tag{4.4}$$

This matrix operation can be carried out by another simple linear analog circuit **T**.

Based upon these two networks we can build the feedback system, which is illustrated in fig.5. It provides for the correction of the sine and cosine components of the first harmonic of the vertical orbit distortion. The output of the 4 PUE's are the input of the Fourier analysis 2 by 4 matrix network **F**. As described above, the output of **F** is the two voltages corresponding to the two Fourier coefficients of $\sin\phi$ and $\cos\phi$ for the vertical feedback with tune 1.20. The linear network with 4 by 2 matrix **T** is used to generate different trim current combinations.

The networks **F** and **T** are determined theoretically in in terms of the Courant-Snyder phases at the detectors and trims. In order that the actual system have two independent channels, we introduce the empirically determined matrix **M** to diagonalize the system, so the transfer matrix from the input of the **M** block to the output of the **F** block is unity, thus providing two independent channels (cosine and sine) for feedback. We use the two boxes g_1, g_2 in fig.5 to represent the servo circuits for the two channels respectively.

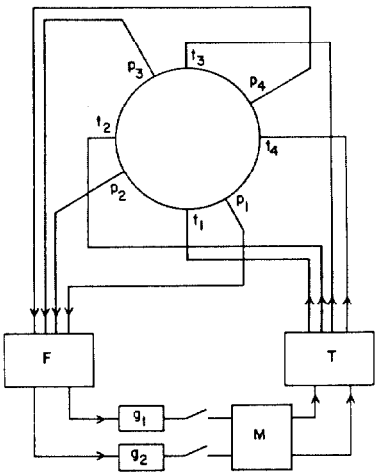

fig.5

Once the loop is closed, we realize the harmonic feedback in real time. The detailed description of the function of **M** is given else where[12,13]. We have found that the network **M** can be determined very accurately by carrying out simple measurements on the storage ring as the feedback system is being installed. The matrix **M** corresponds to a fine adjustment of the system.

An experiment based on this scheme has been carried out on the UV ring[13] The 4 PUE RF detectors (PUE's #1, #7, #13, #19) utilized are uniformly distributed about the ring with their phases separated by $\pi/2$. The 4 trims used are trims #1, #5, #9, #13, also symmetrically distributed about the ring with $\pi/2$ phase separation. The results of the experiment show that the maximum orbit fluctuation around the ring is reduced by a factor between 3 and 4, agrees with the prediction of a numerical simulation. To check the global improvement, the signal power spectrum was measured at 18 PUE locations, with the feedback loop open and closed. When the NSLS booster is ramping, it induces an orbit deviation at its repetition rate of 0.6 Hz. All around UV ring this movement is observed, and the power spectrum exhibits peaks at 0.6 Hz and its harmonics. We plot in fig.6 the amplitude of second harmonic observed at 18 PUE's, comparing the amplitudes with the loop open and closed. The global improvement is clearly demonstrated. For first experiments, the feedback bandwidth was not optimized. This can be significantly improved in future work.

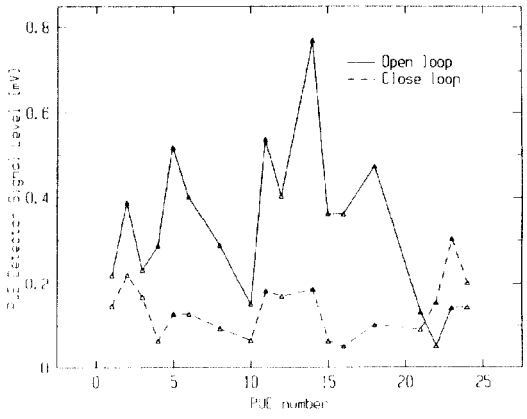

fig.6

The above system can be generalized to more detector and correctors to eliminate more harmonics of orbit distortion near the tune. An 8 detector 8 trim system, correcting 3 harmonics components, will reduce the orbit motion by a factor between 5 to 10. Another system will be built to stabilize X-ray ring orbit. The simulations show that the improved orbit stability should satisfy the tolerance requirements of most beamlines. For those beamlines with tightest tolerances, the stabilized orbit should be able to keep all the detectors for their local bumps within their position dynamic range. When the local bump feedback loops are closed, the harmonic global feedback system will keep the the steering magnets strengths of these local bumps within their range. So the overall performance of the storage rings can be significantly improved.

Acknowledgements

The author wishes to thank S. Krinsky, J. Galayda, E. Johnson for many discussions.

References

[1]L.H.Yu, J.Galayda, L.Ma, BNL-41673
[2]R.Hettel, Nucl. Inst. Meth., 155,A266(1988)
[3]M.Billing, Nucl. Inst. Meth., 144,A266(1988)
[4]R.Biscardi,J.Bittner, in this proceedings
[5]R.O. Hettel, Trans.Nucl.Sci.,Vol. NS-30,2228(1983); J.Tischler and P.L. Hartman, 172 (1980) 67, Nucl. Inst. Meth.; W.Schildkamp, Nucl. Inst. Meth.,(1987)
[6]J.Tischler, P.Hartman,Nucl. Inst. Meth.,172(1980)67; P.Mortazavi,M.Woodle,H.Rarback,D.Shu,M.Howells,Nucl. Inst. Meth., A246(1986)389; F.Wolf,W.Peatman,Nucl. Inst.Meth.,A246(1986)408;S.Heald,Nucl.Inst.Meth., A246(1986)411;
[7]E.Johnson,T.Oversluizen,Third International Conference on Synchrotron Radiation Instrumentation, Tsukuba, Japan (1988)
[8]E.Johnson, private communication
[9]P.Siddon,H.Kraner, NSLS Technical Note 274, BNL (1986)
[10]R.Nawrocky,J.Galayda,D.Klein,O.Singh,L.H.Yu, in this proceedings
[11]R.J.Nawrocky,J.W.Bittner,Li Ma,H.M.Rarback, D. P. Siddons, L. H. Yu, Nucl. Instr. Meth. p.164, A266 (1988)
[12]L.H.Yu,E.Bozoki,J.Galayda,S.Krinsky, G.Vignola, submitted to Nucl Instr. Meth.
[13]L.H.Yu,R.Biscardi,J.Bittner,J.Galyala,S.Krinsky, R. Nawrocky, O. Singh, G. Vignola, in this proceedings
[14]E.D.Courant and H.S.Snyder,Ann.Phy.3,1-48(1958)